Occludin OCEL-domain interactions are required for maintenance and regulation of the tight junction barrier to macromolecular flux

Mary M. Buschmann*, Le Shen*, Harsha Rajapakse, David R. Raleigh, Yitang Wang, Yingmin Wang, Amulya Lingaraju, Juanmin Zha, Elliot Abbott, Erin M. McAuley, Lydia A. Breskin, Licheng Wu, Kenneth Anderson, Jerrold R. Turner, and Christopher R. Weber
Department of Pathology, The University of Chicago, Chicago, IL 60637

ABSTRACT In vitro and in vivo studies implicate occludin in the regulation of paracellular macromolecular flux at steady state and in response to tumor necrosis factor (TNF). To define the roles of occludin in these processes, we established intestinal epithelia with stable occludin knockdown. Knockdown monolayers had markedly enhanced tight junction permeability to large molecules that could be modeled by size-selective channels with radii of ~62.5 Å. TNF increased paracellular flux of large molecules in occludin-sufficient, but not occludin-deficient, monolayers. Complementation using full-length or C-terminal coiled-coil occludin/ELL domain (OCEL)–deficient enhanced green fluorescent protein (EGFP)–occludin showed that TNF-induced occludin endocytosis and barrier regulation both required the OCEL domain. Either TNF treatment or OCEL deletion accelerated EGFP-occludin fluorescence recovery after photobleaching, but TNF treatment did not affect behavior of EGFP-occludin$^{\Delta OCEL}$. Further, the free OCEL domain prevented TNF-induced acceleration of occludin fluorescence recovery, occludin endocytosis, and barrier loss. OCEL mutated within a recently proposed ZO-1–binding domain (K433) could not inhibit TNF effects, but OCEL mutated within the ZO-1 SH3-GuK–binding region (K485/K488) remained functional. We conclude that OCEL-mediated occludin interactions are essential for limiting paracellular macromolecular flux. Moreover, our data implicate interactions mediated by the OCEL K433 region as an effector of TNF-induced barrier regulation.

Tight junctions seal the paracellular space in simple epithelia, such as those lining the lungs, intestines, and kidneys (Anderson *et al.*, 2004; Fanning and Anderson, 2009; Shen *et al.*, 2011). In the intestine, reduced paracellular barrier function is associated with disorders in which increased paracellular flux of ions and molecules contributes to symptoms such as diarrhea, malabsorption, and intestinal

protein loss. Recombinant tumor necrosis factor (TNF) can be used to model this barrier loss in vitro or in vivo (Taylor *et al.*, 1998; Clayburgh *et al.*, 2006), and TNF neutralization is associated with restoration of intestinal barrier function in Crohn's disease (Suenaert *et al.*, 2002). Further, in vivo and in vitro studies of intestinal epithelia show that TNF-induced barrier loss requires myosin light chain kinase (MLCK) activation (Zolotarevsky *et al.*, 2002; Clayburgh *et al.*, 2005, 2006; Ma *et al.*, 2005; Wang *et al.*, 2005). The resulting myosin II regulatory light chain (MLC) phosphorylation drives occludin internalization, which is required for cytokine-induced intestinal epithelial barrier loss (Clayburgh *et al.*, 2005, 2006; Schwarz *et al.*, 2007; Marchiando *et al.*, 2010). In addition, transgenic EGFP-occludin expression in vivo limits TNF-induced depletion of tight junction–associated occludin, barrier loss, and diarrhea (Marchiando *et al.*, 2010). Conversely, in vitro studies show that occludin knockdown limits TNF-induced barrier regulation (Van Itallie *et al.*, 2010). The basis for this discrepancy is not understood.

One challenge is that, despite being identified 20 yr ago (Furuse *et al.*, 1993), the contribution of occludin to tight junction
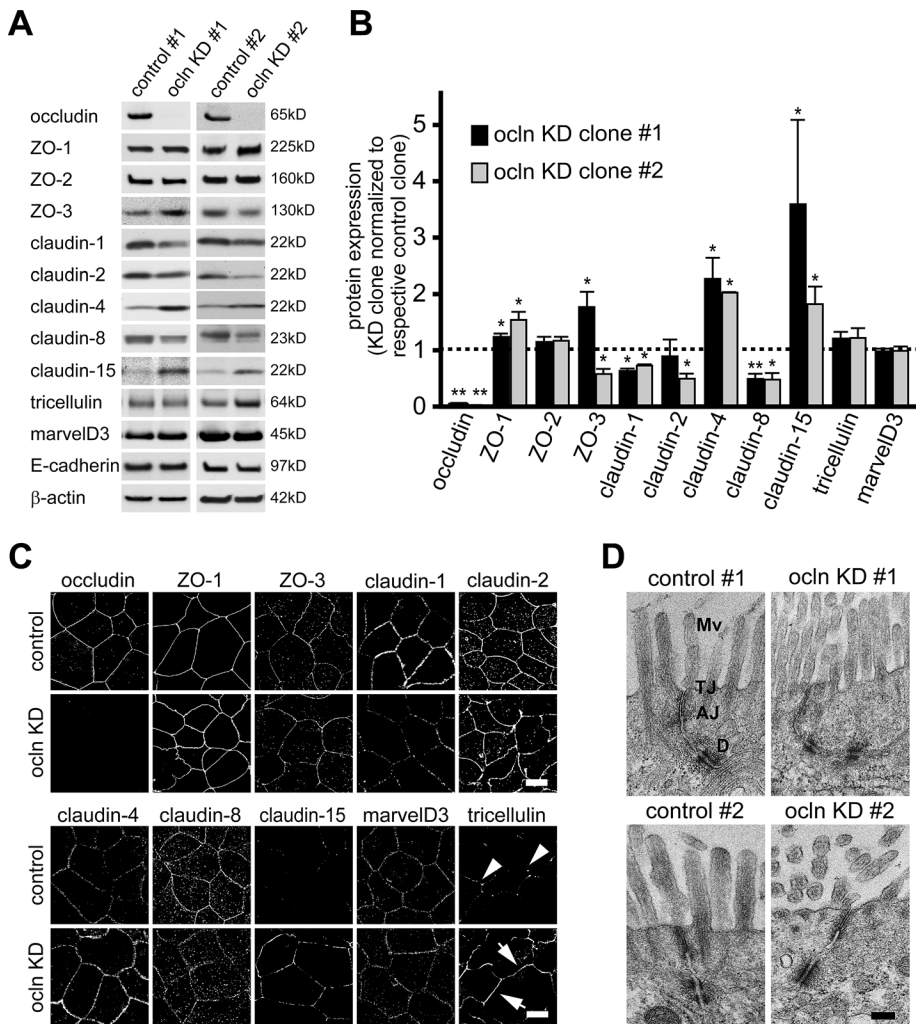
FIGURE 1: Occludin knockdown affects expression of other tight junction proteins. (A) Protein expression assessed by Western blot in two independent occludin-knockdown (ocln KD) or control clones. Claudin-4 and claudin-15 expression consistently increased, whereas claudin-1 and claudin-8 expression decreased. (B) Densitometric analysis of immunoblots (as in A). Average of three separate experiments, each with $n = 3$, of two independent occludin-knockdown clones (black and gray bars), normalized to the paired control lines. (C) Immuno-fluorescence microscopy demonstrates normal tight junction localization of ZO-1, ZO-3, claudin-2, and MarvelD3 in occludin-knockdown lines. Expression of claudin-1, claudin-4, and claudin-15 increased, but localization was not affected. In contrast, tricellulin was redistributed from tricellular tight junctions (arrowheads) to bicellular tight junctions (arrows) after occludin knockdown. Data are representative of two independent control and knockdown clones. Bars, 10 μm. (D) Transmission electron microscopy shows that occludin knockdown did not cause significant ultrastructural alterations of the brush border or apical junctional complex. Representative images from two independent occludin-knockdown clones and corresponding controls. AJ, adherens junction; D, desmosome; Mv, microvilli; TJ, tight junction. Bar, 200 nm. *p <0.05, **p < 0.001.

ZO-1, and claudin-2 that inhibits flux across size- and charge-selective channels termed the pore pathway (Anderson and Van Itallie, 2009; Turner, 2009; Raleigh et al., 2011; Shen et al., 2011). Although this demonstrates that occludin can serve a regulatory role, it does not explain the role of occludin in TNF-induced barrier loss, which increases flux across the size- and charge-nonselective leak pathway (Wang et al., 2005; Weber et al., 2010). In vitro studies, however, do suggest that occludin contributes to leak pathway regulation, as occludin knockdown in either Madin–Darby canine kidney (MDCK) or human intestinal (Caco-2) epithelial monolayers enhances leak pathway permeability (Yu et al., 2005; Al-Sadi et al., 2011; Ye et al., 2011). Taken as a whole, these data suggest that occludin organizes the tight junction to limit leak pathway flux, whereas occludin removal, either by knockdown or endocytosis, enhances leak pathway flux.

To define the mechanisms by which occludin regulates the leak pathway, we analyzed the contributions of occludin, as well as specific occludin domains, to basal and TNF-induced barrier regulation. The data indicate that TNF destabilizes tight junction–associated occludin via interactions mediated by the C-terminal coiled-coil occludin/ELL domain (OCEL). Further, these OCEL-mediated events are required for TNF-induced barrier regulation. Thus these data provide new insight into the structural elements and mechanisms by which occludin regulates leak pathway paracellular flux.

RESULTS

Occludin knockdown alters tight junction protein expression and distribution

The role of occludin in tight junction structure and regulation has been controversial. In part, this reflects the range of approaches used, heterogeneity of cell types studied, and, in cultured monolayers, differences between transient and stable protein knockdown (Yu et al., 2005; Raleigh et al., 2010; Van Itallie et al., 2010; Al-Sadi et al., 2011). To address this, Caco-2$_{BBe}$–derived cell lines with stable expression of a short hairpin RNA (shRNA) specific for occludin and controls were developed. Expression of occludin-targeted shRNA accomplished >95% knockdown of occludin protein expression (Figure 1, A and B). Consistent with a previous analysis of MDCKII cells (Yu et al., 2005), stable occludin knockdown also resulted in reduced claudin-1 and claudin-8 expression, which was observed in independent Caco-2$_{BBe}$–derived occludin-knockdown clones (Figure 1, A and B). Although statistically significant and consistent across clones, increased ZO-1 expression was limited. In contrast, occludin knockdown induced marked increases in claudin-4 and claudin-15

regulation remains incompletely defined. The observation that occludin-knockout mice are able to form paracellular barriers and do not have obvious defects in epidermal, respiratory, or bladder tight junction function (Saitou et al., 2000; Schulzke et al., 2005) led many to conclude that occludin is not essential for tight junction barrier function. It is important to note, however, that barrier regulation in response to stress has not been studied in occludin-deficient animals.

We recently showed that dephosphorylation of occludin serine-408 promotes assembly of a complex composed of occludin,
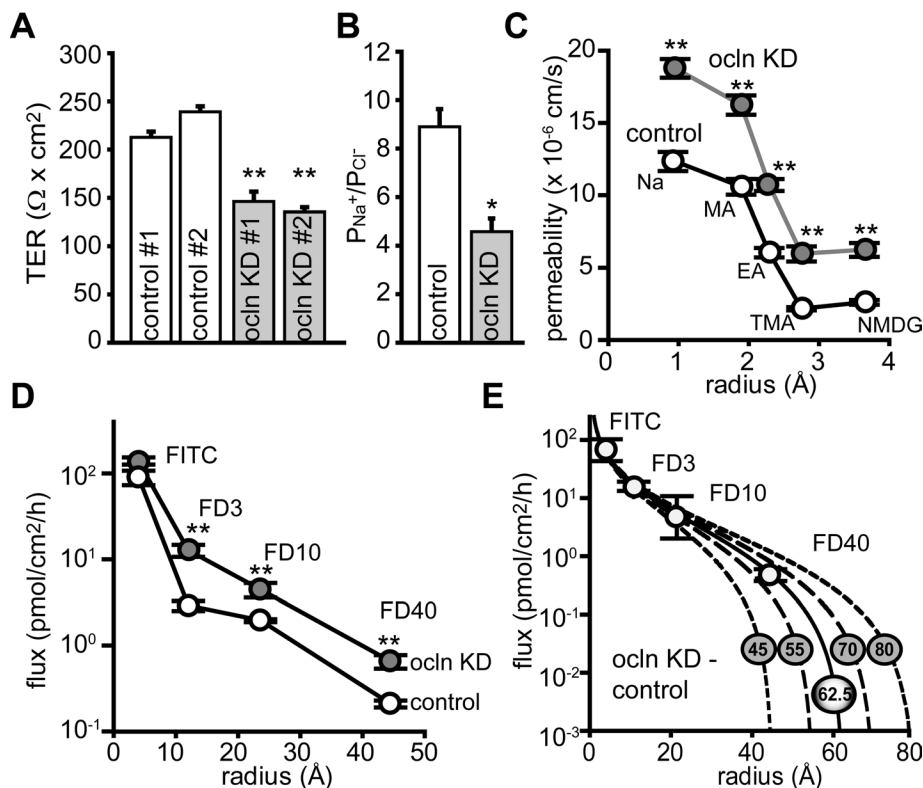
FIGURE 2: Occludin knockdown increases leak pathway permeability. (A) TER of occludin-knockdown monolayers (gray bars) was reduced relative to control monolayers (white bars). Data are the averages of three experiments, each with $n = 4$, from two independent control or occludin-knockdown clones. (B) Charge selectivity, measured as PNa^+/PCl^-, was reduced in occludin-knockdown monolayers (gray bars) relative to control monolayers (white bars). Data are from a representative experiment with $n = 7$. (C) Occludin knockdown increased paracellular flux of cations with radii from 0.95 to 3.65 Å (gray circles) relative to control monolayers (white circles). EA, ethylamine; MA, methylamine; NMDG, N-methyl-D-glucamine. TEA, tetraethylammonium; TMA, tetramethylammonium. Data are the averages of three experiments, each with $n = 4$. (D) Occludin knockdown (gray circles) increased paracellular flux of larger macromolecules (FITC and 3-, 10-, and 40-kDa FITC-dextran) relative to shRNA control monolayers (white circles). Data shown are the averages of two experiments, each with $n = 4$. (E) The net increase in flux induced by occludin knockdown, that is, the difference between the lines in D, is indicated by the white circles and overlaid with solutions of the Renkin sieving equation using size cutoffs of 45, 55, 62.5, 70, or 80 Å. The occludin-dependent component of paracellular macromolecular flux fits the curve modeling a 62.5 Å pore (solid line). *$p < 0.05$, **$p < 0.001$.

expression. Immunofluorescence microscopy confirmed that alterations in claudin protein expression were accompanied by corresponding increases or decreases in the junction-associated pools of these proteins (Figure 1C). Tricellulin was redistributed to bicellular tight junctions of Caco-2$_{BBe}$ monolayers (Figure 1C), consistent with a report in MDCK cells (Ikenouchi et al., 2008). In contrast, occludin knockdown had no effect on MarvelD3 expression or distribution (Figure 1C). Finally, occludin knockdown did not affect the ultrastructure of tight junctions, adherens junctions, or desmosomes (Figure 1D).

Occludin regulates a paracellular leak pathway with radius ~62.5 Å
Occludin has been linked to regulation of both the size- and charge-selective pore pathway and the relatively nonselective leak pathway (Yu et al., 2005; Anderson and Van Itallie, 2009; Marchiando et al., 2010; Van Itallie et al., 2010; Al-Sadi et al., 2011; Raleigh et al., 2011; Shen et al., 2011). Consistent with this, transepithelial electrical

resistance (TER), a measure of overall ion conductance, was reduced in monolayers of both occludin-knockdown lines relative to shRNA controls (Figure 2A). Along with reduced TER, occludin knockdown resulted in a loss of tight junction cation selectivity (Figure 2B). This reflects increased paracellular flux of both Na^+ and Cl^- ions. Thus occludin regulates overall paracellular ion conductance and is essential for maintenance of the cation-selective tight junction barrier that characterizes intestinal epithelia.

Studies of MDCK monolayers suggest that occludin knockdown increases paracellular flux of large cations with radii up to 3.6 Å (Yu et al., 2005). There is disagreement, however, as to whether flux of larger molecules is affected by occludin depletion (Yu et al., 2005; Al-Sadi et al., 2011). We used bi-ionic potential measurements to assess paracellular flux of cations and paracellular macromolecular tracer assays to assess flux of larger molecules with radii up to ~45 Å (Figure 2D). In occludin-knockdown lines, paracellular permeability was increased to molecules of all sizes assayed. These data are consistent with increased permeability of the relatively charge- and size-nonselective leak pathway (Anderson and Van Itallie, 2009; Turner, 2009; Shen et al., 2011).

Although no upper limit has been defined for flux across the leak pathway, this has not been studied in a systematic manner. To define the characteristics of the pathway unmasked by occludin loss, the difference between paracellular flux of control and occludin-knockdown monolayers for molecules with radii up to 45 Å was fit to a Renkin sieving function (Renkin, 1954; Yu et al., 2009). Modeling with pore sizes from 45 to 80 Å (Figure 2E) showed that the increase in paracellular permeability induced by occludin knockdown matched sieving behavior expected for a 62.5 Å pore radius. Thus occludin limits paracellular flux across a size-selective, but charge-nonselective, pathway.

TNF-induced barrier loss requires occludin
A central morphological feature of TNF-induced barrier loss, in vivo and in vitro, is MLCK-dependent occludin endocytosis (Clayburgh et al., 2005, 2006; Marchiando et al., 2010; Wang et al., 2005). This caveolin-1–dependent occludin endocytosis is required for TNF-induced barrier loss (Marchiando et al., 2010). Further, occludin over-expression can limit TNF-induced barrier loss in vivo (Marchiando et al., 2010). One study of MDCKII cells, however, in which TNF paradoxically increased TER, reported that occludin overexpression magnifies and occludin knockdown prevents TNF-induced TER increases (Van Itallie et al., 2010). In Caco-2$_{BBe}$ monolayers, stable occludin knockdown completely prevented TNF-induced barrier loss (Figure 3A). To determine whether this was merely because the occludin-knockdown monolayers had lower initial TER, we analyzed eight independent occludin-knockdown and four shRNA control
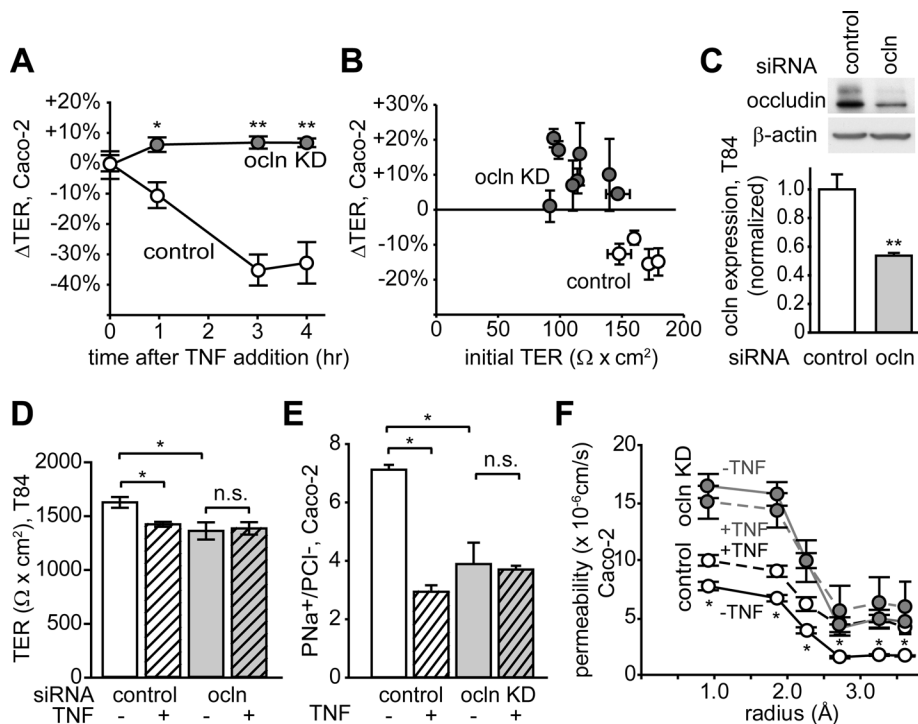
FIGURE 3: Occludin is required for TNF-induced barrier loss. (A) TNF reduced the TER of shRNA control Caco-2$_{BBe}$ (white circles) but not occludin-knockdown (ocln KD; gray circles) Caco-2$_{BBe}$ monolayers. Data are the average of three independent experiments, each with $n = 10$. (B) Protection from TNF-induced barrier loss was independent of initial TER. Each data point represents a separate occludin-knockdown (ocln KD, gray circles, eight clones) or shRNA control (white circles, four clones) clone. Data are from a representative experiment with $n = 4$ monolayers (for each point). (C) Transient siRNA-mediated occludin knockdown (gray bar) reduced occludin expression by $46 \pm 2\%$ relative to control siRNA (white bar) in T84 monolayers. Data are from a representative experiment with $n = 6$. (D) TNF (hatched bars) reduced TER of siRNA control (white bars) but not occludin-knockdown (gray bars) T84 monolayers. Data are representative of three independent experiments, each with $n = 3$. (E) TNF (hatched bars) did not significantly alter the charge selectivity (PNa+/PCl−) of occludin-knockdown (ocln KD) monolayers (gray bars). Data are representative of three independent experiments, each with $n = 3$. (F). TNF (dashed lines) increased paracellular permeability of cations with radii from 0.95 to 3.65 Å in control (white circles) but not occludin-knockdown (gray circles) monolayers. Data are representative of four independent experiments, each with $n = 4$. *$p < 0.05$, **$p < 0.001$.

pathway barrier regulation in intestinal epithelia both in vitro and in vivo.

The above data suggest that the effects of occludin knockdown on paracellular permeability may be synonymous with the increased leak pathway flux induced by TNF (Clayburgh et al., 2005; Turner, 2009; Van Itallie et al., 2009; Yu et al., 2010; Shen et al., 2011). Along with a reduction in TER, TNF treatment reduced charge selectivity, that is, PNa+/PCl−, of shRNA control but not occludin-knockdown monolayers (Figure 3E). Further, whereas TNF increased paracellular permeability of cations with radii from 0.95 to 3.6 Å in shRNA control monolayers, no effect was detected in occludin-knockdown monolayers (Figure 3F). The independent effects of TNF and occludin knockdown on paracellular permeability of larger molecules, that is, those with radii >2.5 Å, were similar (Figure 3F), suggesting that the barrier loss induced by TNF-induced occludin removal from the tight junction is redundant with that occurring after occludin knockdown. Relative to TNF treatment, however, occludin knockdown induced far greater increases in paracellular permeability of cations with radii <2.5 Å (Figure 3F). Thus, although the effects of TNF and occludin knockdown on barrier function overlap, they are not identical.

Occludin functions distal to MLCK activation in TNF-induced barrier loss

It is possible that occludin-dependent changes in claudin protein expression might contribute to the protection of occludin-knockdown cells from TNF-induced barrier loss (Colegio et al., 2002; Wada et al., 2013). The distributions of MarvelD3 and claudin-2, however, were unaffected by TNF in both shRNA control and occludin-knockdown monolayers (Figure 4A). In addition, TNF did not affect expression of tight or adherens junction proteins in either shRNA control or occludin-knockdown monolayers (Figure 4B). Finally, TNF did not alter tricellulin distribution in either shRNA control or occludin-knockdown monolayers, suggesting that tricellulin redistribution was not responsible for the barrier loss observed in occludin-expressing monolayers.

Occludin has been implicated in the regulation of cell surface receptor signaling (Barrios-Rodiles et al., 2005). TNF signals through TNF receptor 2 (TNFR2) to activate myosin light chain kinase (MLCK) to drive myosin regulatory light chain (MLC) phosphorylation and barrier loss (Zolotarevsky et al., 2002; Clayburgh et al., 2005; Wang et al., 2006; Su et al., 2013). Thus, if occludin is required for TNFR2 signaling, this could explain the failure of TNF to induce barrier loss in occludin-knockdown monolayers. To test this hypothesis, we assessed TNF-induced events upstream of barrier loss in occludin-knockdown monolayers. The irregular ZO-1 undulations that are characteristic of in vitro and in vivo TNF-induced MLCK activation (Clayburgh et al., 2005; Wang et al., 2005), as well as genetically regulated MLC phosphorylation

Caco-2$_{BBe}$ clones. Despite varying initial TER values across these lines, TNF induced TER loss in all occludin-expressing monolayers but not in occludin-knockdown monolayers (Figure 3B; $p < 0.001$). Of importance, this was true even when occludin-knockdown and control monolayers with similar initial TER values were compared.

We considered the hypothesis that the divergent effects of TNF on TER in MDCKII and Caco-2$_{BBe}$ monolayers reflected differences in cell type, that is, dog kidney versus human intestine. To test this, we transiently knocked down occludin in a different human intestinal epithelial line, T84 (Figure 3C). This reduced TER (Figure 3D) in a manner similar to that observed after stable occludin knockdown in Caco-2$_{BBe}$ monolayers, despite incomplete suppression, as is typical after transient small interfering RNA (siRNA) transfection (Clayburgh et al., 2004; Al-Sadi et al., 2011). Further, occludin knockdown in T84 monolayers blocked TNF-induced TER loss (Figure 3D). Thus both the TER loss induced by TNF and the occludin dependence of this effect are similar in T84 and Caco-2$_{BBe}$ intestinal epithelial monolayers. Together with the observation that intestinal epithelial–specific occludin overexpression limits TNF-induced increases in paracellular macromolecular flux (Marchiando et al., 2010), these data suggest that occludin is critical for leak
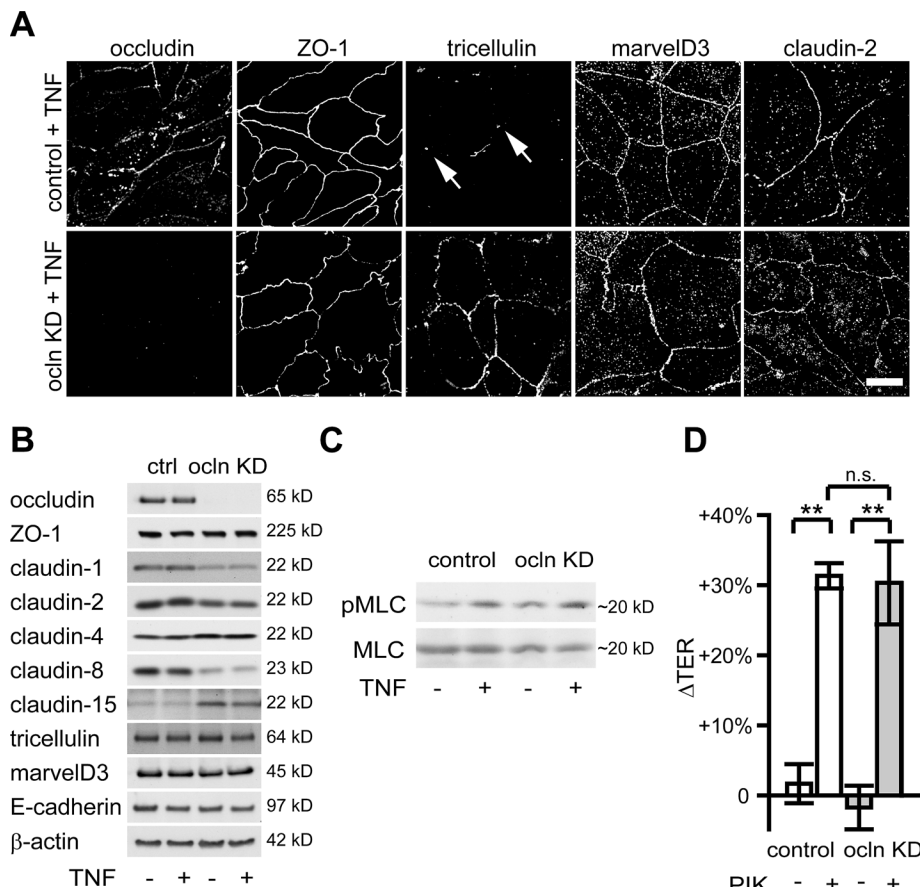
FIGURE 4: Occludin is not required for TNF-induced MLC phosphorylation or TNF-independent, MLCK-mediated tight junction regulation. (A) TNF induced occludin internalization and ZO-1 profile undulations in shRNA control monolayers. Although occludin internalization was not detected in occludin-knockdown monolayers, TNF-induced ZO-1 profile undulations were present. Arrows show tricellulin at the tricellular junction of TNF-treated shRNA control monolayers. Bar, 10 μm. Results are typical of three independent experiments. (B) TNF treatment did not affect expression of other tight junction proteins in shRNA control or occludin-knockdown clones. β-Actin was used as a loading control. Results are representative of three experiments, each with $n = 3$. (C) TNF induced similar increases in phosphorylated MLC (pMLC) in shRNA control or occludin-knockdown clones. Total MLC is shown as a loading control. Results are representative of three experiments, each with $n = 3$, $p < 0.05$. (D) PIK (250 μM) caused similar TER increases in shRNA control (white bars) or occludin-knockdown (gray bars) monolayers with active Na$^+$-glucose cotransport. Results are representative of three experiments, each with $n = 4$. **$p < 0.001$.

permeable inhibitor of MLCK (PIK; Zolotarevsky et al., 2002; Owens et al., 2005) reversed Na$^+$-glucose cotransport–induced tight junction regulation and increased TER similarly in shRNA control and occludin-knockdown monolayers (Figure 4D). These data show that, despite resistance to TNF-induced barrier loss, an intact MLCK-dependent regulatory pathway is present in occludin-knockdown monolayers. Therefore, MLCK-mediated barrier regulation can occur by occludin-independent as well as by occludin-dependent mechanisms that lead to distinct alterations in paracellular flux.

The OCEL domain is required for occludin trafficking and occludin-dependent barrier function

Occludin is a tetraspanning transmembrane protein with a short N-terminal cytoplasmic tail, two extracellular loops, and a long C-terminal cytoplasmic tail (Furuse et al., 1993; Wong, 1997). The extracellular loops and the C-terminal tail have all been shown to mediate interprotein interactions (Furuse et al., 1994; Chen et al., 1997; Van Itallie and Anderson, 1997; Wong and Gumbiner, 1997; Wittchen et al., 1999; Nusrat et al., 2000, 2005; Barrios-Rodiles et al., 2005; Li et al., 2005; Elias et al., 2009; Raleigh et al., 2011). Moreover, the C-terminal cytoplasmic tail has been implicated in both occludin targeting to the tight junction and development of barrier function (Balda et al., 1996, 2000; Bamforth et al., 1999). The C-terminal cytoplasmic tail includes a 107–amino acid occludin/ELL domain, termed the OCEL domain, that is necessary for interactions between occludin and ZO-1, actin, and multiple kinases and may also mediate homotypic occludin–occludin interactions (Furuse et al., 1994; Fanning et al., 1998; Wittchen et al., 1999; Nusrat et al., 2000, 2005; Li et al., 2005). To determine whether OCEL-mediated interactions are involved in occludin-dependent, TNF-induced barrier loss, we inducibly expressed EGFP-occludin and EGFP-occludin$^{\Delta OCEL}$ in occludin-knockdown and shRNA control Caco-2$_{BBe}$ cells (Figure 5A). EGFP-occludin was correctly targeted to the tight junction, as well as to lateral membranes (Figure 5B), likely as a result of overexpression, similar to the distribution of EGFP-occludin in transgenic mice (Marchiando et al., 2010). In contrast, EGFP-occludin$^{\Delta OCEL}$ was primarily found along lateral membranes, with only a small tight junction–associated pool (Figure 5B), consistent with a previous study (Furuse et al., 1994).

EGFP-occludin expression increased TER of occludin-knockdown and shRNA control monolayers in a dose-dependent manner (Figure 5C). This fully reversed the barrier defect induced by occludin knockdown, since TER of occludin-knockdown and shRNA control monolayers was similar at the highest levels of EGFP-occludin expression (Figure 5C). In contrast, neither EGFP-occludin$^{\Delta OCEL}$ nor EGFP expression increased TER to the same extent as

(Shen et al., 2006), were induced by TNF in both shRNA control and occludin-knockdown monolayers (Figure 4A; compare to Figure 1C). TNF-induced MLC phosphorylation was also comparable in shRNA control and occludin-knockdown monolayers (Figure 4C). We next considered the hypothesis that the inability of TNF to induce barrier loss in occludin-knockdown monolayers reflects disruption of regulatory linkages between the tight junction and cytoskeleton, which would be consistent with reports that occludin binds to and regulates perijunctional actin (Atsumi et al., 1999; Wittchen et al., 1999; Kuwabara et al., 2001). To test this, we examined physiological Na$^+$-glucose cotransport–induced tight junction regulation (Madara and Pappenheimer, 1987; Jodal et al., 1994), which, like TNF-induced tight junction regulation, requires MLCK (Turner et al., 1997). However, Na$^+$-glucose cotransport–induced tight junction regulation is size selective and does not involve altered trafficking or endocytosis of occludin (Jodal et al., 1994; Turner et al., 1997; Yu et al., 2010). The highly specific
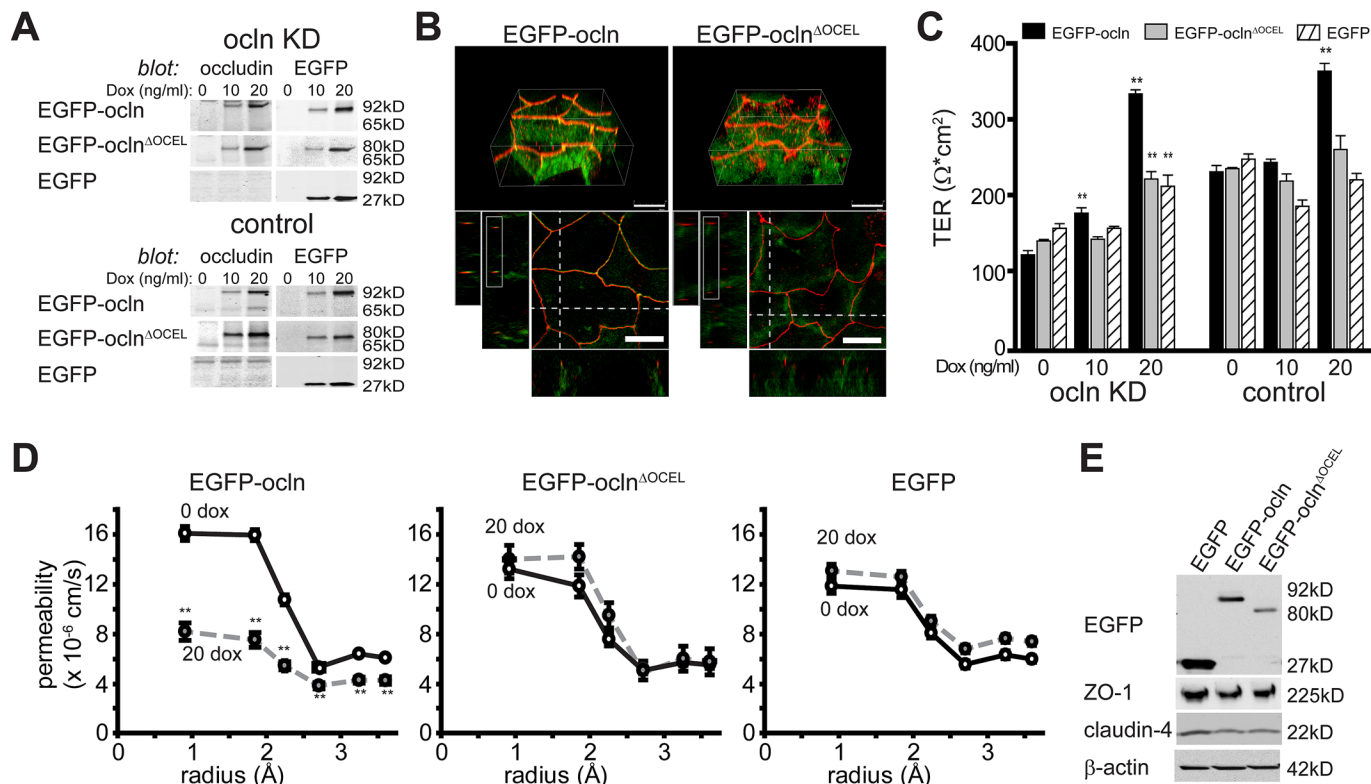
FIGURE 5: The occludin OCEL domain is required for TNF-induced barrier loss. (A) Doxycycline-inducible (tet-on) EGFP-occludin (EGFP-ocln), EGFP-occludin$^{\Delta OCEL}$ (EGFP-ocln$^{\Delta OCEL}$), and free EGFP were expressed in occludin-knockdown (ocln KD) and shRNA control (control) monolayers. EGFP-occludin was expressed at levels similar to endogenous occludin at 10 ng/ml doxycycline. Results are representative of four experiments, each with $n = 4$. (B) Three-dimensional reconstructions (top; bar, 15 μm), and an xy plane image at the level of the tight junction (bar, 10 μm), along with corresponding xz and yz sections. Expression of EGFP-occludin or EGFP-occludin$^{\Delta OCEL}$ in occludin-knockdown monolayers did not alter ZO-1 distribution at the tight junction. EGFP-occludin was localized at the junction and along lateral membranes, but EGFP-occludin$^{\Delta OCEL}$ was found only at lateral membranes. Results are representative of five experiments. (C) Expression of EGFP-occludin, but not EGFP-occludin$^{\Delta OCEL}$ or free EGFP, in occludin KD monolayers restored TER. At 10 and 20 ng/ml doxycycline, EGFP-occludin expression significantly increased TER of occludin-knockdown monolayers. Results are representative of four experiments, each with $n = 4$. (D) Expression of EGFP-occludin, but not EGFP-occludin$^{\Delta OCEL}$ or EGFP, in occludin KD monolayers restored tight junction size selectivity. Results are representative of three experiments, each with $n \geq 3$. (E) Expression of EGFP-occludin, but not EGFP-occludin$^{\Delta OCEL}$ or EGFP, in occludin KD monolayers reduced claudin-4 expression. β-Actin is shown as a loading control. Data are representative of three independent experiments, each with $n = 3$. **$p < 0.001$.

EGFP-occludin in either occludin-knockdown or shRNA control monolayers (Figure 5C).

In addition to restoring overall TER, EGFP-occludin expression restored paracellular size selectivity of occludin-knockdown monolayers (Figure 5D). In contrast, neither EGFP-occludin$^{\Delta OCEL}$ nor EGFP expression had any effect on paracellular size selectivity (Figure 5D). Of interest, expression of either EGFP-occludin or EGFP-occludin$^{\Delta OCEL}$, but not free EGFP, reduced claudin-4 expression to levels similar to those in shRNA control cells (Figure 5E). In contrast, effects of EGFP-occludin or EGFP-occludin$^{\Delta OCEL}$ expression on claudin-1, claudin-8, and claudin-15 expression were inconsistent across clones. These results indicate that occludin, through the OCEL domain, plays a critical role in regulating size-selectivity and barrier function in intestinal epithelia. Further, because claudin-4 expression was reduced to normal levels by EGFP-occludin or EGFP-occludin$^{\Delta OCEL}$ expression despite the failure of EGFP-occludin$^{\Delta OCEL}$ expression to restore overall barrier function (TER) and size selectivity, claudin-4 up-regulation is unlikely to be responsible for the observed effects of occludin knockdown on TER.

TNF-induced occludin internalization and barrier loss require OCEL-domain function

To determine whether the C-terminal occludin OCEL domain is required for TNF-induced occludin internalization and barrier regulation, we expressed EGFP-occludin or EGFP-occludin$^{\Delta OCEL}$ in occludin-knockdown monolayers. Like endogenous occludin, EGFP-occludin was internalized after TNF treatment (Figure 6A). Moreover, EGFP-occludin expression restored the barrier loss response after TNF treatment (Figure 6B). In contrast to EGFP-occludin, EGFP-occludin$^{\Delta OCEL}$ was not internalized after TNF treatment but remained localized to lateral membranes (Figure 6A). Further, occludin-knockdown monolayers expressing EGFP-occludin$^{\Delta OCEL}$ remained resistant to TNF-induced barrier loss (Figure 6B). Thus the C-terminal occludin OCEL domain is required for both TNF-induced occludin endocytosis and tight junction barrier regulation.

The OCEL domain stabilizes junctional occludin

Previous studies showed that, despite little change in steady-state distribution, alterations in dynamic behaviors of tight junction proteins can have profound effects on barrier function (Yu et al., 2010;
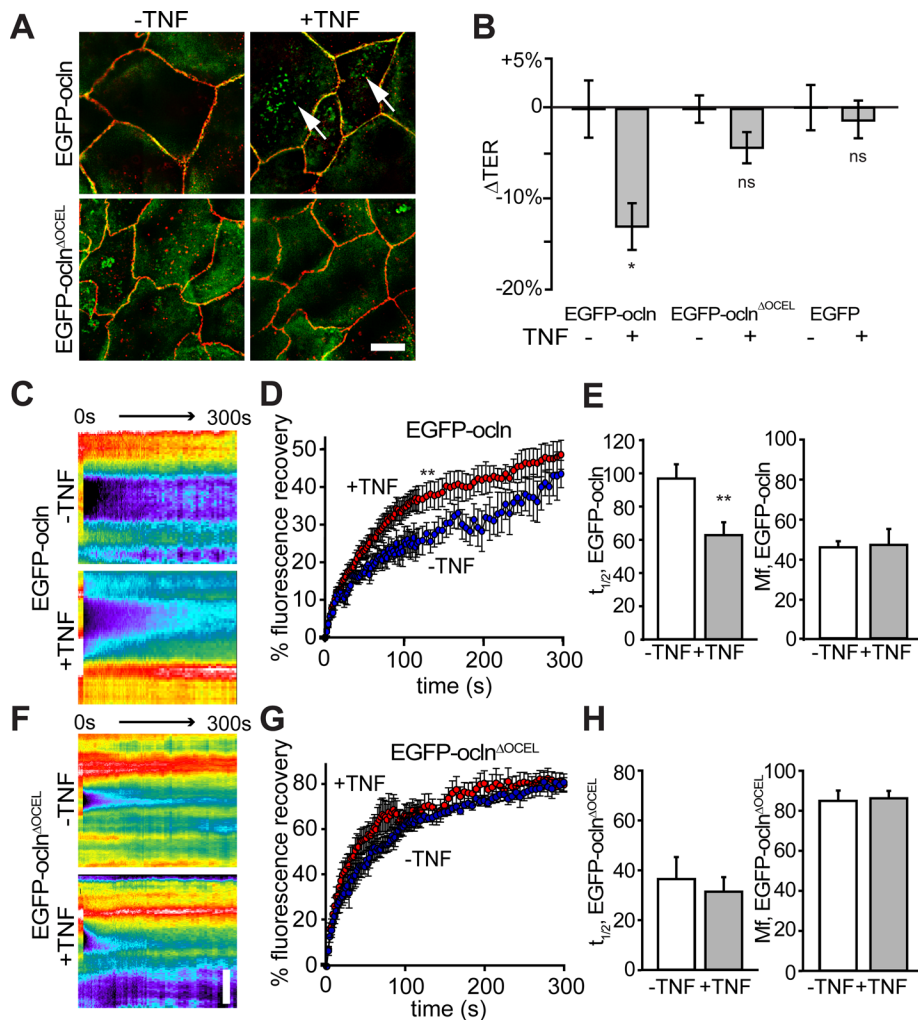
FIGURE 6: The OCEL domain is required for TNF-dependent regulation of occludin stability at the tight junction. (A) TNF treatment induced EGFP-occludin, but not EGFP-occludin$^{\Delta OCEL}$, internalization. EGFP-occludin–containing vesicles (green) were readily detected after TNF treatment (arrows). EGFP-occludin$^{\Delta OCEL}$–containing vesicles (green) were not seen. ZO-1 (red) was detected by immunostaining. Bar, 10 µm. Results are representative of four independent experiments. (B) Occludin-knockdown monolayers were resensitized to TNF-induced barrier loss after EGFP-occludin expression. In contrast, occludin-knockdown monolayers expressing EGFP or EGFP-occludin$^{\Delta OCEL}$ were resistant to TNF. Results are representative of four experiments, each with $n = 4$. (C, F) FRAP kymographs of occludin-knockdown monolayers expressing EGFP-occludin or EGFP-occludin$^{\Delta OCEL}$ 4 h after TNF treatment. Results are representative of $n \geq$ 8 recordings per condition. Bar, 5 µm. (D, G) EGFP-occludin or EGFP-occludin$^{\Delta OCEL}$ fluorescence recovery curves for control (blue circles) and TNF-treated (red circles) monolayers. Results are averages from two experiments with at least eight recordings per condition. (E, H) Mobile fractions and $t_{1/2}$ for control or TNF-treated monolayers expressing EGFP-occludin or EGFP-occludin$^{\Delta OCEL}$. Results are averages of two experiments with at least eight recordings per condition. *$p < 0.05$, **$p < 0.001$.

Raleigh et al., 2011). To determine whether TNF-associated occludin redistribution and barrier loss are associated with changes in occludin dynamic behavior, we assessed occludin fluorescence recovery after photobleaching (FRAP). EGFP-occludin was expressed in occludin-knockdown monolayers to avoid artifacts due to protein interactions with endogenous occludin. After TNF treatment, the time required for half-maximal fluorescence recovery ($t_{1/2}$) of tight junction–associated EGFP-occludin significantly decreased (Figure 6, C–E). In contrast, the mobile fraction was not affected. Thus TNF promotes an increase in the rate of occludin exchange, that is, diffusion within the membrane, without affecting the size of the pool

available for exchange, that is, the mobile fraction. This increased diffusion rate might facilitate concentration of occludin at the nascent endocytosis sites that have been described in vivo (Marchiando et al., 2010).

The FRAP behavior of EGFP-occludin$^{\Delta OCEL}$ expressed in occludin-knockdown monolayers was markedly different from that of full-length EGFP-occludin (Figure 6). The $t_{1/2}$ was reduced, indicating an increased rate of fluorescence recovery (Figure 6). In addition, the occludin$^{\Delta OCEL}$ mobile fraction was significantly increased relative to full-length occludin (Figure 6), suggesting that the OCEL domain anchors occludin at the tight junction in a manner that restricts both rate and extent of recovery. In contrast to full-length occludin, however, the $t_{1/2}$ of occludin$^{\Delta OCEL}$ was unaffected by TNF treatment (Figure 6). The failure of TNF to affect the rate of occludin$^{\Delta OCEL}$ exchange may reflect the fact that OCEL-domain deletion had already reduced $t_{1/2}$ to that of full-length occludin in TNF-treated monolayers. However, the mobile fraction of occludin$^{\Delta OCEL}$ was elevated relative to that of full-length occludin and was unaffected by TNF treatment. This suggests that the OCEL domain regulates the size of the occludin mobile fraction independent of TNF while also regulating the rate of occludin exchange in a TNF-dependent manner. These data support the hypothesis that TNF activates signaling events that destabilize OCEL domain–dependent protein interactions at the tight junction and that this is a mechanism of TNF-induced barrier loss.

The occludin OCEL domain acts as a dominant-negative regulator to prevent TNF-induced barrier loss

It remains possible that basal barrier loss caused by occludin knockdown explains the inability of TNF to induce further barrier loss. This could also explain why occludin$^{\Delta OCEL}$ expression, which did not correct basal barrier function, failed to restore TNF sensitivity. It might then follow that the TNF resistance of occludin-knockdown and occludin$^{\Delta OCEL}$-expressing monolayers merely reflects global barrier defects rather than a specific defect in TNF-induced tight junction regulation. Alternatively, TER and FRAP data suggest that interactions mediated by the OCEL domain are required for TNF-induced barrier loss. If occludin OCEL-domain interactions are critical regulators of occludin stability and sensitivity to TNF-mediated endocytosis, expression of the OCEL domain alone would be expected to bind OCEL-domain partners, block OCEL-mediated occludin interactions, and prevent TNF-induced barrier loss. The effect of EGFP-tagged OCEL domain (EGFP-OCEL) expression on TNF-induced barrier loss was therefore assessed in wild-type Caco-2$_{BBe}$ monolayers (Figure 7A), that is, those expressing endogenous

A

	EGFP	EGFP-OCEL
EGFP-OCEL		— 40kD
EGFP	—	27kD
β-actin	—	— 42kD

B

EGFP	+	-	+	-
EGFP-OCEL	-	+	-	+
TNF	-	-	+	+
occludin					65kD
EGFP-OCEL					40kD
pMLC					20kD
ZO-1					225kD
claudin-4					22kD
claudin-8					23kD
claudin-15					22kD
β-actin					42kD

C

ΔTER

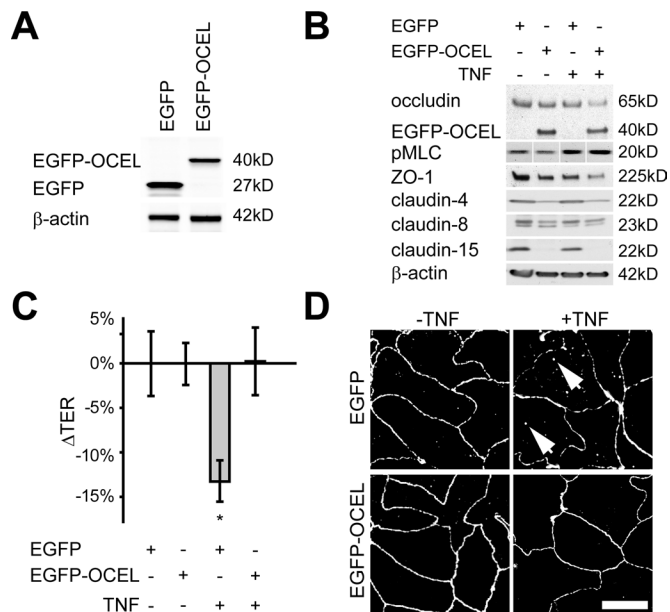| EGFP	+	-	+	-
EGFP-OCEL	-	+	-	+
TNF	-	-	+	+

D

-TNF   +TNF

EGFP

EGFP-OCEL

FIGURE 7: The OCEL domain acts as a dominant-negative effector to prevent TNF-mediated barrier loss. (A) EGFP and EGFP fused to the occludin OCEL domain (EGFP-OCEL) were stably expressed at similar levels. Proteins were separated by SDS–PAGE and blotted with anti-GFP or anti–β-actin antibodies. Results are representative of four experiments, each with n = 3. (B) EGFP-OCEL was expressed at levels similar to endogenous occludin. Proteins were separated by SDS–PAGE and blotted with antibodies to occludin (occludin and EGFP-OCEL) or other proteins indicated. Claudin-4, -8, and -15 expression was reduced in EGFP-OCEL–expressing cells, regardless of TNF treatment. TNF induced a modest but nonsignificant reduction in endogenous occludin expression, similar to that reported previously (Wang et al., 2005), which was not affected by EGFP-OCEL expression. Results are representative of three experiments, each with n = 3. (C) EGFP-OCEL, but not EGFP, expression prevented TNF-induced TER loss. Results are the average of five experiments, each with n = 4. (D) EGFP-OCEL expression prevented TNF-induced endocytosis of endogenous (full-length) occludin. Occludin vesicles were present in TNF-treated monolayers expressing EGFP (arrows). Endogenous occludin was detected by immunostaining. Images are maximum projections assembled from z stacks and are representative of three independent experiments. Bar, 10 μm. *p < 0.05.

occludin. Neither EGFP nor EGFP-OCEL localized to the tight junction. EGFP-OCEL expression did reduce expression of claudin-4, claudin-8, and claudin-15 (Figure 7B). This was similar to the reduced claudin-8 expression induced by occludin knockdown. In contrast, the effects of EGFP-OCEL expression and occludin knockdown diverged for claudin-4 and claudin-15 expression. These data suggest that some signaling functionality may be retained by the free OCEL domain.

EGFP-OCEL expression prevented TNF-induced barrier loss (Figure 7C). Further, EGFP-OCEL expression also blocked TNF-induced internalization of endogenous occludin (Figure 7D). These effects were not due to OCEL-mediated disruption of TNF-induced MLC phosphorylation or TNF-induced changes in expression of other tight junction proteins (Figure 7B). The free OCEL domain can therefore function as a dominant-negative regulator that prevents TNF-induced occludin internalization and barrier regulation.

Lysine 433 regulates OCEL interactions that are critical to TNF-induced occludin destabilization and endocytosis

Specific amino acids have been implicated in ZO-1 binding and tight junction barrier function by creating charged regions within the occludin OCEL domain (Li et al., 2005; Sundstrom et al., 2009; Tash et al., 2012). To test whether OCEL binding to ZO-1 or other proteins is important for barrier regulation, we created OCEL mutants with charge-reversing mutations at lysine 433 (K433D) or lysines 485 and 488 (K485D/K488D). These were selected for comparison because they have been proposed to define separate OCEL-binding faces for distinct ZO-1 domains (Li et al., 2005; Reese et al., 2007; Tash et al., 2012).

Similar to EGFP-OCEL, mCherry-OCEL and OCEL point mutants had no effect on expression (Figure 8A) or localization (Figure 8B) of endogenous occludin or ZO-1, and all OCEL constructs were diffusely distributed throughout the cytoplasm. To determine whether disruption of protein interactions by OCEL-domain expression affects occludin FRAP behavior before or after TNF treatment, we coexpressed EGFP-occludin with mCherry, mCherry-OCEL, mCherry-OCEL[433], or mCherry-OCEL[485/488]. The pool of EGFP-occludin available for exchange, that is, the mobile fraction, was not affected by mCherry, mCherry-OCEL, mCherry-OCEL[485/488], or mCherry-OCEL[433] expression (Figure 8C). In contrast, effects of expressing different OCEL-domain constructs on the $t_{1/2}$ of EGFP-occludin recovery diverged; $t_{1/2}$ was reduced by mCherry-OCEL, unaffected by mCherry-OCEL[485/488], and increased by mCherry-OCEL[433] (Figure 8C). Similar to the results shown in Figure 6, TNF treatment accelerated EGFP-occludin exchange, that is, reduced $t_{1/2}$, in monolayers expressing mCherry (Figure 8D). In contrast, expression of either mCherry-OCEL or mCherry-OCEL[485/488] blocked TNF effects on the $t_{1/2}$ of EGFP-occludin recovery (Figure 8C). TNF reduced the $t_{1/2}$ of EGFP-occludin recovery in monolayers expressing mCherry-OCEL[433] (Figure 8D), although $t_{1/2}$ was still far greater than that in monolayers expressing mCherry. Thus K433 within the occludin OCEL is essential for the protein interactions that mediate the dominant-negative effect of OCEL on TNF-induced $t_{1/2}$ decreases, whereas K485 and K488 are not required. Further, the dramatic effect of OCEL K433D on basal $t_{1/2}$ suggests that interactions mediated by this site might also play other roles in regulating occludin dynamic behavior.

As shown in Figure 7, EGFP-OCEL expression can prevent internalization of endogenous occludin after TNF treatment. Similarly, mCherry-OCEL prevented TNF-induced occludin internalization (Figure 8E). In a manner that correlates directly with the TNF-induced changes in occludin FRAP behavior, expression of mCherry-OCEL[485/488], but not mCherry or mCherry-OCEL[433], also prevented occludin internalization. Thus, like changes in FRAP behavior, K433-dependent interactions are critical to TNF-induced occludin internalization, whereas K485- and K488-mediated interactions are dispensable.

DISCUSSION

The functions of occludin have been difficult to discern. Whereas an occludin-knockout mouse displays a complex phenotype, the absence of intestinal or renal defects has led some to conclude that occludin is not essential to tight junction barrier function (Saitou et al., 2000). Other data, however, suggest that occludin is a critical component of the tight junction, and both in vivo and in vitro studies indicate that occludin is a critical regulator of tight junction barrier function (Marchiando et al., 2010; Van Itallie et al., 2010).

Our data showing that occludin loss reduces TER and enhances permeability of a paracellular leak pathway with a radius of ~62.5 Å
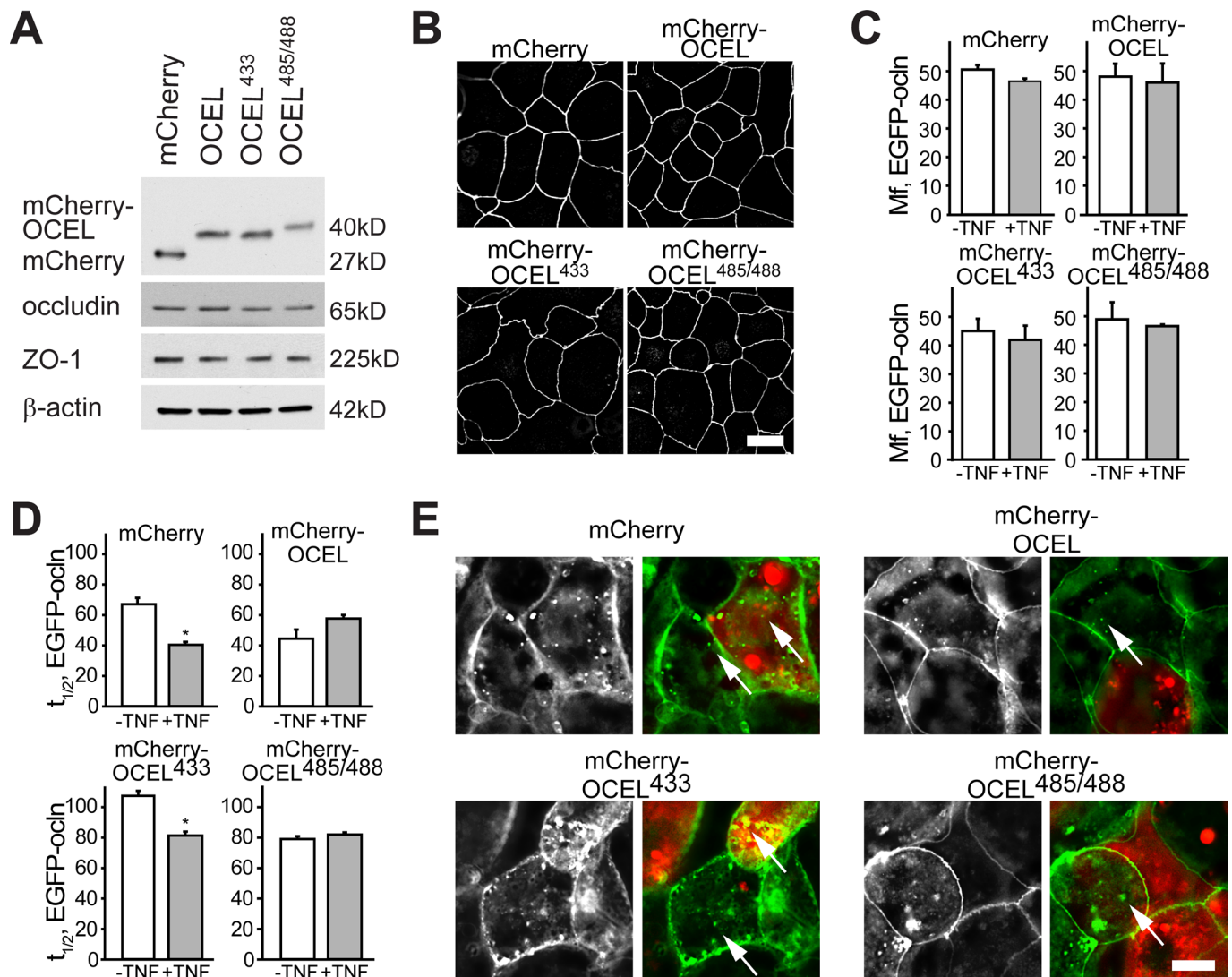
FIGURE 8: Lysine 433 regulates OCEL interactions and is critical to TNF-induced barrier loss and occludin endocytosis. (A) Expression of mCherry, mCherry-OCEL, or mCherry-OCEL mutants (indicated residues are lysines that were mutated to aspartic acids) does not affect expression of endogenous occludin or ZO-1. Fusion proteins were detected with an anti-DsRed antibody that also recognizes mCherry. Results are representative of three experiments, each with $n = 3$. (B) Expression of mCherry, mCherry-OCEL, or mCherry-OCEL mutants did not affect ZO-1 localization at the tight junction. Images are representative of two independent experiments. Bar, 10 μm. (C) Expression of mCherry, mCherry-OCEL, or mCherry-OCEL mutants did not affect the EGFP-occludin mobile fraction. Results are averages of two experiments with at least eight recordings per condition. (D) Expression of mCherry-OCEL or mCherry-OCEL mutants, but not mCherry, altered the EGFP-occludin $t_{1/2}$. Only mCherry-OCEL or mCherry-OCEL[485/488] blocked TNF-induced reduction of EGFP-occludin $t_{1/2}$. Results are averages of two independent experiments, with at least eight recordings per condition. (E) TNF induced accumulation of intracellular EGFP-occludin (green) vesicles (arrows) in cells that did not express mCherry or mCherry-OCEL proteins (red). Occludin vesicles were also present in cells expressing mCherry or mCherry-OCEL[433] but not in cells expressing Cherry-OCEL or mCherry-OCEL[485/488]. Images are representative of three independent experiments. Bar, 10 μm. *$p < 0.05$.

contrasts with previous stable knockdown in MDCK monolayers (Yu *et al.*, 2005) and transient partial knockdown in the relatively undifferentiated Caco-2 parental cell line (Al-Sadi *et al.*, 2011). Nevertheless, we do confirm published data showing that occludin plays an essential role in TNF-induced barrier loss (Marchiando *et al.*, 2010; Van Itallie *et al.*, 2010). In contrast to previous work in MDCKII monolayers, which respond to TNF by increasing both TER and paracellular macromolecular flux, we show that occludin knockdown in well-differentiated Caco-2$_{BBe}$ monolayers prevents TNF-induced TER decreases. Further, we show that interactions mediated by the occludin OCEL domain are necessary for TNF-induced occludin mo-

bilization, internalization, and barrier loss. Finally, our data indicate that the critical residues within the OCEL lie within a recently proposed second ZO-1–binding face rather than the positively charged OCEL face that binds to ZO-1 SH3-GuK.

Occludin-dependent leak pathway flux is size selective

In recent years the tight junction barrier has been shown to allow paracellular flux by at least two distinct pathways (Anderson and Van Itallie, 2009; Turner, 2009; Shen *et al.*, 2011). These pathways can be classified as a high-capacity, charge- and size-selective pore pathway that is modulated by claudin proteins and can be activated by either

IL-13–induced or transgenic claudin-2 expression (Van Itallie et al., 2008; Weber et al., 2010), and a low-capacity, charge- and size-non-selective leak pathway that requires ZO-1 for maintenance and can be regulated by TNF via MLCK- and caveolin-1–dependent occludin endocytosis. Occludin has been implicated in the regulation of both pathways. Although differences exist, we show here that occludin knockdown induces leak pathway barrier defects that are similar to those induced by TNF. It is therefore reasonable to tentatively define leak pathway flux as the increased permeability occurring after occludin knockdown. We applied a macromolecular sieving model (Renkin, 1954) to define this as increased paracellular flux across a pathway with a functional radius of ~62.5 Å. This is far larger than the pores formed by claudins but does suggest that rather than representing breaks or other gross defects, occludin-dependent leak pathway flux occurs via large channels within the tight junction. The molecular identity of leak pathway channels remains to be determined, but the data suggest that occludin prevents these channels from forming or opening. Alternatively, tricellulin redistribution in occludin-knockdown monolayers raises the possibility that these channels may be formed or otherwise regulated by tricellulin (Ikenouchi et al., 2008; Krug et al., 2009).

Expression of claudin-1, claudin-4, claudin-8, and claudin-15 was affected by occludin knockdown. These changes may, in part, explain the marked increase in pore pathway small-molecule flux in occludin-knockdown cell lines. For example, increased claudin-15 expression would likely increase paracellular permeability to small cations. It should have increased PNa^+/PCl^-, whereas we observed a decrease in PNa^+/PCl^- after occludin knockdown. Further, claudin-4 up-regulation would be expected to reduce pore pathway flux (Van Itallie et al., 2001). Moreover, both EGFP-occludin and EGFP-occludin$^{\Delta OCEL}$ expression restored claudin-4 expression to control levels, yet only EGFP-occludin corrected barrier function defects. Finally, OCEL-domain expression, which also blocked TNF-induced barrier loss, resulted in a third pattern of altered claudin expression. It is therefore difficult to define whether or how these changes contribute to barrier defects in occludin-knockdown monolayers. Nevertheless, this is an area in need of further investigation, as decreased claudin-1 and increased claudin-4 expression were also noted in occludin-knockdown MDCK cells (Yu et al., 2005), and increased claudin-4 expression has been reported in MDCK cells expressing mutant occludin (Balda et al., 2000).

TNF-mediated barrier loss is occludin dependent
Our demonstration that barrier function is not reduced by TNF in occludin-knockdown Caco-2$_{BBe}$ intestinal epithelia is consistent with a previous report in MDCK cells (Van Itallie et al., 2010). In contrast, our in vivo analyses showed that high levels of EGFP-occludin expression in intestinal epithelium prevented TNF-induced barrier loss, likely because tight junction–associated occludin pools were maintained (Marchiando et al., 2010). In contrast, occludin overexpression in MDCK monolayers amplified TNF effects. Thus, whereas studies of Caco-2 monolayers and mouse intestine are concordant, they are not entirely consistent with studies using MDCK cells. This may reflect tissue of origin or other differences, as we and others have noted divergence in cytoskeletal mechanisms of barrier regulation in MDCK monolayers relative to Caco-2 monolayers or intestinal mucosa.

Our data show that the OCEL domain, which mediates interactions with ZO-1 and other regulatory proteins, is necessary for occludin-dependent maintenance and regulation of barrier function. These observations expand on previous studies indicating an important functional role for the C-terminal tail of occludin (Balda et al., 1996; Bamforth et al., 1999). We explored the essential roles

of the C-terminal occludin tail by three distinct approaches. First, OCEL deletion enhanced both the rate and extent of occludin exchange at steady state. Second, in contrast to full-length occludin, OCEL-deficient occludin was unable to restore TNF-induced barrier regulation in occludin-knockdown monolayers. This result contrasts sharply with a previous study showing increased TER after expression of a C-terminal deletion occludin mutant in MDCK monolayers (Balda et al., 1996). This difference may reflect the presence of endogenous occludin along with mutant occludin in the previous work, differences between occludin mutants studied, or use of distinct cell lines and types. Finally, expression of the OCEL domain as a free dominant-negative protein blocked TNF-induced barrier loss, as well as mobilization and internalization of full-length occludin. The latter effects were abrogated by a charge-reversing mutation within a recently described second OCEL-binding face that may bind to ZO-1 U5 or U6 (Tash et al., 2012) but not by mutations within the positively charged face that binds to the ZO-1 SH3-GuK domain (Li et al., 2005). Although the significance of this observation is not clear, it is interesting that the positively charged OCEL face and S490, whose phosphorylation and ubiquitination have been linked to vascular endothelial growth factor–induced occludin endocytosis in endothelial cells (Murakami et al., 2009, 2012) are adjacent to residues 485 and 488 but at some distance from the K433 site. Thus K433 may define a second OCEL site that regulates occludin trafficking and endocytosis.

Taken together, our data demonstrate that OCEL-mediated interactions of occludin within the tight junction complex regulate paracellular flux of macromolecules with radii up to ~62.5 Å and suggest that the leak pathway might be size selective. The data also provide new insight into the mechanisms by which TNF triggers occludin internalization to regulate barrier function. Finally, the findings indicate that disruption of specific OCEL-mediated interactions, possibly with ZO-1, may be an effective means to prevent cytokine-induced barrier loss in intestinal disease.

MATERIALS AND METHODS
Cell culture and cytokine treatment
Caco-2$_{BBe}$ and T84 cells were maintained and plated on Transwell supports as described previously (Wang et al., 2005; Weber et al., 2010). Before TNF treatment, monolayers were cultured with interferon-γ (10 ng/ml, added to basolateral media; R&D Systems, Minneapolis, MN) for 18–24 h (Wang et al., 2006). TNF (5 ng/ml, R&D Systems) was then added to the basolateral media. PIK (250 μM) was applied apically (Zolotarevsky et al., 2002).

Analysis of barrier function
A standard current-clamp approach was used to measure TER of cultured monolayers, as described previously (Turner et al., 1997). NaCl dilution potentials and PNa^+/PCl^- were determined as described previously (Weber et al., 2010). Bi-ionic potentials were measured by replacing basal Na^+ (radius, 0.95 Å) with larger cations, specifically methylamine (MA^+; 1.9 Å), ethylamine (EA^+; 2.3 Å), tetramethylammonium (TMA^+; 2.8 Å), tetraethylammonium (TEA^+; 3.3 Å), and N-methyl-D-glucamine ($NMDG^+$; 3.7 Å; Sigma-Aldrich, St. Louis, MO). Absolute Na^+ permeability (PNa^+) was calculated using the Kimizuka and Koketsu equation, as previously described (Kimizuka and Koketsu, 1964; Yu et al., 2009). Flux of fluorescein isothiocyanate (FITC; 0.1 mg/ml), 3 kDa FITC-dextran (1 mg/ml), 10 kDa FITC-dextran (2.5 mg/ml), and 40 kDa FITC-dextran (3.5 mg/ml) conjugates (Invitrogen, Carlsbad, CA) was assessed in the apical-to-basolateral direction over 2 h, as described previously (Wang et al., 2005).

Modeling

The difference in flux between control and occludin-knockdown monolayers was fit to a Renkin sieving model (Renkin, 1954; Yu et al., 2009). This model assumes that the permeating molecules are spherical and that the tight junction barrier is cylindrical with a defined radius. In these fits, two parameters were allowed to vary: a constant reflecting the number, density, and pathway open probability, and a fixed radius (Yu et al., 2009).

Occludin knockdown

pSUPER (OligoEngine, Seattle, WA) containing the occludin targeting sequence 5′-GTGAAGAGTACATGGCTGC-3′ with inserted blasticidin-resistant cassette (Yu et al., 2005; Raleigh et al., 2010, 2011) was used to stably transfect Caco-2$_{BBe}$ cells stably expressing SGLT1 (Turner et al., 1997). Controls for each were generated by stable transfection of the pSUPER vector. Several knockdown and control clones were isolated. For transient occludin knockdown in T84 monolayers, siRNA duplexes (ON-TARGETplus; ThermoFisher, Dharmacon, Lafayette, CO) targeting the same sequence as the shRNA or siRNA controls (ON-TARGETplus non-targeting siRNA #1; ThermoFisher, Dharmacon) were transfected using Lipofectamine 2000 (Invitrogen), as previously described (Weber et al., 2010). Monolayers were assayed 4 d after plating.

Immunoblotting

Monolayers were lysed and scraped from Transwell supports in SDS-extraction buffer (50 mM Tris, pH 8.8, 2% SDS, 5 mM EDTA) and then reduced in Laemmli sample buffer and alkylated with iodoacetamide. SDS–PAGE and transfer to polyvinylidene fluoride membrane were performed as described previously (Wang et al., 2006). Targets of interest were probed with primary antibodies against claudin-1, claudin-2, claudin-4, claudin-8, occludin, C-terminal tricellulin, ZO-1, ZO-2, ZO-3 (Invitrogen), β-actin (Sigma-Aldrich), MarvelD3, pMLC (Ser-19; Cell Signaling Technology, Beverly, MA), E-cadherin (Cell Signaling Technology), mCherry (anti-DsRed; Clontech, Mountain View, CA), and total MLC, followed by horseradish peroxidase–conjugated secondary antibodies, as described (Schwarz et al., 2007; Raleigh et al., 2010; Weber et al., 2010). Protein was detected by chemiluminescence. Densitometry was performed using ImageJ software (National Institutes of Health, Bethesda, MD). For all studies, densitometry values were first normalized to β-actin and then to control monolayers.

Immunofluorescence staining and microscopy

To preserve intracellular vesicles, monolayers were fixed at –20°C with methanol and then cross-linked with bis(sulfosuccinimidyl)suberate (Shen and Turner, 2005). The only exceptions were staining for MarvelD3 and tricellulin, which required fixation with 1% paraformaldehyde (Raleigh et al., 2010). Immunofluorescence staining used GFP, claudin-1, claudin-2, claudin-4, claudin-8, claudin-15, occludin, tricellulin, ZO-1, and ZO-2 antibodies (Invitrogen), as well as anti-MarvelD3 polyclonal antisera (Raleigh et al., 2010), followed by species-specific secondary antisera conjugated to Alexa Fluor 488 or Alexa Fluor 594 (Invitrogen). Images were collected using a DM4000 epifluorescence microscope (Leica, Wetzlar, Germany) equipped with a 63× Plan Apochromat 1.32 numerical aperture (NA) oil immersion objective, Retiga EXi camera (QImaging, Surrey, Canada), and Chroma ET bandpass filter cubes controlled by MetaMorph 7 (Molecular Devices, Sunnyvale, CA). Z-stacks were collected at 0.2 μm intervals and deconvolved with Autoquant X3 (Media Cybernetics, Bethesda, MD) for 10 iterations. Three-dimensional reconstructions were generated in Autoquant X3. MetaMorph

7.7 was used to generate xz and yz plane images. For electron microscopy studies, monolayers were fixed with 2.5% glutaraldehyde and 4% paraformaldehyde in 0.1 M sodium cacodylate buffer, dehydrated, and embedded in Spurr. Images were collected at 15,000× using a scanning transmission electron microscope (Tecnai F30; FEI, Hillsboro, OR).

Fluorescent proteins

EGFP-occludin was expressed as described previously (Yu et al., 2010). siRNA-evading mutations were generated by site-directed mutagenesis, as described previously (Raleigh et al., 2011). EGFP-occludin$^{\Delta OCEL}$ was created by introducing a premature stop sequence after codon 415. An EGFP-occludin OCEL-domain (416–522) fusion protein was expressed from the EF1α promoter. For doxycycline induction studies, piggyBAC-TREtight plasmids were generated by cloning a human EF1α promoter and TetOn3G expression cassette between the inverted terminal repeats of the piggyBAC plasmid (System Biosciences, Mountain View, CA). EGFP, EGFP-occludin, or EGFP-occludin$^{\Delta OCEL}$ constructs (as described) were then cloned into the multiple cloning site of this plasmid. For coexpression of EGFP-occludin and mCherry-OCEL or point mutants, mCherry, mCherry-OCEL, mCherry-OCEL^{433}, or mCherry-OCEL$^{485/488}$ were expressed from an EF1α promoter and transiently expressed in Caco-2$_{BBe}$ cells stably transfected with piggyBAC-TREtight-EGFP-occludin.

Fluorescence recovery after photobleaching

FRAP was performed as described previously (Yu et al., 2010; Raleigh et al., 2011). Monolayers were imaged in Hank's balanced salt solution on a 37°C temperature-controlled stage. Fluorescence bleaching and imaging were performed using an epifluorescence microscope (Leica DM4000) with a MicroPoint system (Photonic Instruments, St. Charles, IL) and 63× U-V-I 0.9 NA water immersion objective. Images were collected using MetaMorph software until postbleach steady-state fluorescence intensity was achieved. Raw data were aligned, and mean fluorescence of bleached regions was quantified using MetaMorph. Background fluorescence was subtracted, and signals were normalized to prebleach levels. Double-exponential fits allowed calculation of mobile fraction and half-time of fluorescence recovery.

Statistical analysis

All data are presented as mean ± SEM unless otherwise specified. Student's unpaired t test was used to compare means, with statistical significance taken as *$p < 0.05$ and **$p < 0.001$, unless otherwise stated. Regression analysis and analysis of variance were performed using SPSS software (IBM, Armonk, NY).

REFERENCES

Al-Sadi R, Khatib K, Guo S, Ye D, Youssef M, Ma T (2011). Occludin regulates macromolecule flux across the intestinal epithelial tight junction barrier. Am J Physiol Gastrointest Liver Physiol 300, G1054–G1064.

Anderson JM, Van Itallie CM (2009). Physiology and function of the tight junction. Cold Spring Harb Perspect Biol 1, a002584.

Anderson JM, Van Itallie CM, Fanning AS (2004). Setting up a selective barrier at the apical junction complex. Curr Opin Cell Biol 16, 140–145.

Atsumi S et al. (1999). Occludin modulates organization of perijunctional circumferential actin in rat endothelial cells. Med Electron Microsc 32, 11–19.

Balda MS, Flores-Maldonado C, Cereijido M, Matter K (2000). Multiple domains of occludin are involved in the regulation of paracellular permeability. J Cell Biochem 78, 85–96.

Balda MS, Whitney JA, Flores C, Gonzalez S, Cereijido M, Matter K (1996). Functional dissociation of paracellular permeability and transepithelial electrical resistance and disruption of the apical-basolateral intramembrane diffusion barrier by expression of a mutant tight junction membrane protein. J Cell Biol 134, 1031–1049.

Bamforth SD, Kniesel U, Wolburg H, Engelhardt B, Risau W (1999). A dominant mutant of occludin disrupts tight junction structure and function. J Cell Sci 112, 1879–1888.

Barrios-Rodiles M et al. (2005). High-throughput mapping of a dynamic signaling network in mammalian cells. Science 307, 1621–1625.

Chen Y, Merzdorf C, Paul DL, Goodenough DA (1997). COOH terminus of occludin is required for tight junction barrier function in early Xenopus embryos. J Cell Biol 138, 891–899.

Clayburgh DR, Barrett TA, Tang Y, Meddings JB, Van Eldik LJ, Watterson DM, Clarke LL, Mrsny RJ, Turner JR (2005). Epithelial myosin light chain kinase-dependent barrier dysfunction mediates T cell activation-induced diarrhea in vivo. J Clin Invest 115, 2702–2715.

Clayburgh DR, Musch MW, Leitges M, Fu YX, Turner JR (2006). Coordinated epithelial NHE3 inhibition and barrier dysfunction are required for TNF-mediated diarrhea in vivo. J Clin Invest 116, 2682–2694.

Clayburgh DR, Rosen S, Witkowski ED, Wang F, Blair S, Dudek S, Garcia JG, Alverdy JC, Turner JR (2004). A differentiation-dependent splice variant of myosin light chain kinase, MLCK1, regulates epithelial tight junction permeability. J Biol Chem 279, 55506–55513.

Colegio OR, Van Itallie CM, McCrea HJ, Rahner C, Anderson JM (2002). Claudins create charge-selective channels in the paracellular pathway between epithelial cells. Am J Physiol Cell Physiol 283, C142–C147.

Elias BC, Suzuki T, Seth A, Giorgianni F, Kale G, Shen L, Turner JR, Naren A, Desiderio DM, Rao R (2009). Phosphorylation of Tyr-398 and Tyr-402 in occludin prevents its interaction with ZO-1 and destabilizes its assembly at the tight junctions. J Biol Chem 284, 1559–1569.

Fanning AS, Anderson JM (2009). Zonula occludens-1 and -2 are cytosolic scaffolds that regulate the assembly of cellular junctions. Ann NY Acad Sci 1165, 113–120.

Fanning AS, Jameson BJ, Jesaitis LA, Anderson JM (1998). The tight junction protein ZO-1 establishes a link between the transmembrane protein occludin and the actin cytoskeleton. J Biol Chem 273, 29745–29753.

Furuse M, Hirase T, Itoh M, Nagafuchi A, Yonemura S, Tsukita S, Tsukita S (1993). Occludin: a novel integral membrane protein localizing at tight junctions. J Cell Biol 123, 1777–1788.

Furuse M, Itoh M, Hirase T, Nagafuchi A, Yonemura S, Tsukita S (1994). Direct association of occludin with ZO-1 and its possible involvement in the localization of occludin at tight junctions. J Cell Biol 127, 1617–1626.

Ikenouchi J, Sasaki H, Tsukita S, Furuse M (2008). Loss of occludin affects tricellular localization of tricellulin. Mol Biol Cell 19, 4687–4693.

Jodal M, Fihn B-M, Sjøqvist A (1994). Effect of glucose on passive transport of extracellular probes across the rat small intestinal epithelium in vivo. Gastroenterology 107, A241.

Kimizuka H, Koketsu K (1964). Ion transport through cell membrane. J Theor Biol 6, 290–305.

Krug SM, Amasheh S, Richter JF, Milatz S, Gunzel D, Westphal JK, Huber O, Schulzke JD, Fromm M (2009). Tricellulin forms a barrier to macromolecules in tricellular tight junctions without affecting ion permeability. Mol Biol Cell 20, 3713–3724.

Kuwabara H, Kokai Y, Kojima T, Takakuwa R, Mori M, Sawada N (2001). Occludin regulates actin cytoskeleton in endothelial cells. Cell Struct Funct 26, 109–116.

Li Y, Fanning AS, Anderson JM, Lavie A (2005). Structure of the conserved cytoplasmic C-terminal domain of occludin: identification of the ZO-1 binding surface. J Mol Biol 352, 151–164.

Ma TY, Boivin MA, Ye D, Pedram A, Said HM (2005). Mechanism of TNF-alpha modulation of Caco-2 intestinal epithelial tight junction barrier: role of myosin light-chain kinase protein expression. Am J Physiol Gastrointest Liver Physiol 288, G422–G430.

Madara JL, Pappenheimer JR (1987). Structural basis for physiological regulation of paracellular pathways in intestinal epithelia. J Membr Biol 100, 149–164.

Marchiando AM et al. (2010). Caveolin-1-dependent occludin endocytosis is required for TNF-induced tight junction regulation in vivo. J Cell Biol 189, 111–126.

Murakami T, Felinski EA, Antonetti DA (2009). Occludin phosphorylation and ubiquitination regulate tight junction trafficking and vascular endothelial growth factor-induced permeability. J Biol Chem 284, 21036–21046.

Murakami T, Frey T, Lin C, Antonetti DA (2012). Protein kinase cbeta phosphorylates occludin regulating tight junction trafficking in vascular endothelial growth factor-induced permeability in vivo. Diabetes 61, 1573–1583.

Nusrat A, Brown GT, Tom J, Drake A, Bui TT, Quan C, Mrsny RJ (2005). Multiple protein interactions involving proposed extracellular loop domains of the tight junction protein occludin. Mol Biol Cell 16, 1725–1734.

Nusrat A, Chen JA, Foley CS, Liang TW, Tom J, Cromwell M, Quan C, Mrsny RJ (2000). The coiled-coil domain of occludin can act to organize structural and functional elements of the epithelial tight junction. J Biol Chem 275, 29816–29822.

Owens SE, Graham WV, Siccardi D, Turner JR, Mrsny RJ (2005). A strategy to identify stable membrane-permeant peptide inhibitors of myosin light chain kinase. Pharm Res 22, 703–709.

Raleigh DR et al. (2011). Occludin S408 phosphorylation regulates tight junction protein interactions and barrier function. J Cell Biol 193, 565–582.

Raleigh DR, Marchiando AM, Zhang Y, Shen L, Sasaki H, Wang Y, Long M, Turner JR (2010). Tight junction-associated MARVEL proteins MarvelD3, tricellulin, and occludin have distinct but overlapping functions. Mol Biol Cell 21, 1200–1213.

Reese ML, Dakoji S, Bredt DS, Dotsch V (2007). The guanylate kinase domain of the MAGUK PSD-95 binds dynamically to a conserved motif in MAP1a. Nat Struct Mol Biol 14, 155–163.

Renkin EM (1954). Filtration, diffusion, and molecular sieving through porous cellulose membranes. J Gen Physiol 38, 225–243.

Saitou M, Furuse M, Sasaki H, Schulzke JD, Fromm M, Takano H, Noda T, Tsukita S (2000). Complex phenotype of mice lacking occludin, a component of tight junction strands. Mol Biol Cell 11, 4131–4142.

Schulzke JD, Gitter AH, Mankertz J, Spiegel S, Seidler U, Amasheh S, Saitou M, Tsukita S, Fromm M (2005). Epithelial transport and barrier function in occludin-deficient mice. Biochim Biophys Acta 1669, 34–42.

Schwarz BT, Wang F, Shen L, Clayburgh DR, Su L, Wang Y, Fu YX, Turner JR (2007). LIGHT signals directly to intestinal epithelia to cause barrier dysfunction via cytoskeletal and endocytic mechanisms. Gastroenterology 132, 2383–2394.

Shen L, Black ED, Witkowski ED, Lencer WI, Guerriero V, Schneeberger EE, Turner JR (2006). Myosin light chain phosphorylation regulates barrier function by remodeling tight junction structure. J Cell Sci 119, 2095–2106.

Shen L, Turner JR (2005). Actin depolymerization disrupts tight junctions via caveolae-mediated endocytosis. Mol Biol Cell 16, 3919–3936.

Shen L, Weber CR, Raleigh DR, Yu D, Turner JR (2011). Tight junction pore and leak pathways: a dynamic duo. Annu Rev Physiol 73, 283–309.

Su L et al. (2013). TNFR2 activates MLCK-dependent tight junction dysregulation to cause apoptosis-mediated barrier loss and experimental colitis. Gastroenterology 145, 407–415.

Suenaert P, Bulteel V, Lemmens L, Noman M, Geypens B, Van Assche G, Geboes K, Ceuppens JL, Rutgeerts P (2002). Anti-tumor necrosis factor treatment restores the gut barrier in Crohn's disease. Am J Gastroenterol 97, 2000–2004.

Sundstrom JM, Tash BR, Murakami T, Flanagan JM, Bewley MC, Stanley BA, Gonsar KB, Antonetti DA (2009). Identification and analysis of occludin phosphosites: a combined mass spectrometry and bioinformatics approach. J Proteome Res 8, 808–817.

Tash BR, Bewley MC, Russo M, Keil JM, Griffin KA, Sundstrom JM, Antonetti DA, Tian F, Flanagan JM (2012). The occludin and ZO-1 complex, defined by small angle X-ray scattering and NMR, has implications for modulating tight junction permeability. Proc Natl Acad Sci USA 109, 10855–10860.

Taylor CT, Dzus AL, Colgan SP (1998). Autocrine regulation of epithelial permeability by hypoxia: role for polarized release of tumor necrosis factor alpha. Gastroenterology 114, 657–668.

Turner JR (2009). Intestinal mucosal barrier function in health and disease. Nat Rev Immunol 9, 799–809.

Turner JR, Rill BK, Carlson SL, Carnes D, Kerner R, Mrsny RJ, Madara JL (1997). Physiological regulation of epithelial tight junctions is associated

with myosin light-chain phosphorylation. Am J Physiol 273, C1378–C1385.

Van Itallie CM, Anderson JM (1997). Occludin confers adhesiveness when expressed in fibroblasts. J Cell Sci 110, 1113–1121.

Van Itallie CM, Fanning AS, Bridges A, Anderson JM (2009). ZO-1 stabilizes the tight junction solute barrier through coupling to the perijunctional cytoskeleton. Mol Biol Cell 20, 3930–3940.

Van Itallie CM, Fanning AS, Holmes J, Anderson JM (2010). Occludin is required for cytokine-induced regulation of tight junction barriers. J Cell Sci 2844–2852.

Van Itallie CM, Holmes J, Bridges A, Gookin JL, Coccaro MR, Proctor W, Colegio OR, Anderson JM (2008). The density of small tight junction pores varies among cell types and is increased by expression of claudin-2. J Cell Sci 121, 298–305.

Van Itallie C, Rahner C, Anderson JM (2001). Regulated expression of claudin-4 decreases paracellular conductance through a selective decrease in sodium permeability. J Clin Invest 107, 1319–1327.

Wada M, Tamura A, Takahashi N, Tsukita S (2013). Loss of claudins 2 and 15 from mice causes defects in paracellular Na(+) flow and nutrient transport in gut and leads to death from malnutrition. Gastroenterology 144, 369–380.

Wang F, Graham WV, Wang Y, Witkowski ED, Schwarz BT, Turner JR (2005). Interferon-gamma and tumor necrosis factor-alpha synergize to induce intestinal epithelial barrier dysfunction by up-regulating myosin light chain kinase expression. Am J Pathol 166, 409–419.

Wang F, Schwarz BT, Graham WV, Wang Y, Su L, Clayburgh DR, Abraham C, Turner JR (2006). IFN-gamma-induced TNFR2 expression is required for TNF-dependent intestinal epithelial barrier dysfunction. Gastroenterology 131, 1153–1163.

Weber CR, Raleigh DR, Su L, Shen L, Sullivan EA, Wang Y, Turner JR (2010). Epithelial myosin light chain kinase activation induces mucosal

interleukin-13 expression to alter tight junction ion selectivity. J Biol Chem 285, 12037–12046.

Wittchen ES, Haskins J, Stevenson BR (1999). Protein interactions at the tight junction. Actin has multiple binding partners, and ZO-1 forms independent complexes with ZO-2 and ZO-3. J Biol Chem 274, 35179–35185.

Wong V (1997). Phosphorylation of occludin correlates with occludin localization and function at the tight junction. Am J Physiol 273, C1859–C1867.

Wong V, Gumbiner BM (1997). A synthetic peptide corresponding to the extracellular domain of occludin perturbs the tight junction permeability barrier. J Cell Biol 136, 399–409.

Ye D, Guo S, Al-Sadi R, Ma TY (2011). MicroRNA regulation of intestinal epithelial tight junction permeability. Gastroenterology 141, 1323–1333.

Yu AS, Cheng MH, Angelow S, Gunzel D, Kanzawa SA, Schneeberger EE, Fromm M, Coalson RD (2009). Molecular basis for cation selectivity in claudin-2-based paracellular pores: identification of an electrostatic interaction site. J Gen Physiol 133, 111–127.

Yu AS, McCarthy KM, Francis SA, McCormack JM, Lai J, Rogers RA, Lynch RD, Schneeberger EE (2005). Knockdown of occludin expression leads to diverse phenotypic alterations in epithelial cells. Am J Physiol Cell Physiol 288, C1231–C1241.

Yu D, Marchiando AM, Weber CR, Raleigh DR, Wang Y, Shen L, Turner JR (2010). MLCK-dependent exchange and actin binding region-dependent anchoring of ZO-1 regulate tight junction barrier function. Proc Natl Acad Sci USA 107, 8237–8241.

Zolotarevsky Y, Hecht G, Koutsouris A, Gonzalez DE, Quan C, Tom J, Mrsny RJ, Turner JR (2002). A membrane-permeant peptide that inhibits MLC kinase restores barrier function in in vitro models of intestinal disease. Gastroenterology 123, 163–172.